Journal of Alloys and Compounds 745 (2018) 84–89

Contents lists available at ScienceDirect

Journal of Alloys and Compounds

journal homepage: http://www.elsevier.com/locate/jalcom

The characterization of Ce/Pr-doped YAG phosphor ceramic for the white LEDs

Yanru Tang [a, b], Shengming Zhou [a, *], Xuezhuan Yi [a], Deming Hao [a], Xiuchen Shao [a, c], Jie Chen [a, c]

[a] Key Laboratory of Materials for High Power Laser, Shanghai Institute of Optics and Fine Mechanics, Chinese Academy of Sciences, Shanghai 201800, China
[b] University of Chinese Academy of Sciences, Beijing 100049, China
[c] Shanghai Tech University, Shanghai 201210, China

ARTICLE INFO

Article history:
Received 19 October 2017
Received in revised form
6 February 2018
Accepted 11 February 2018
Available online 17 February 2018

Keywords:
WLED
Ce:Pr:YAG
CRI
Luminous efficacy
Composite phase ceramic phosphor

ABSTRACT

Ce/Pr -doped YAG (Ce:Pr:YAG) transparent ceramics are fabricated by the vacuum sintering. The crystal structure and morphology, the energy transfer between Ce^{3+} and Pr^{3+}, and luminescence properties are measured and discussed. The effect of the micrographs of the starting powders and the doping contents of Ce^{3+} and Pr^{3+} ions on the microstructure of YAG ceramic is also exhibited. In the photoluminescence spectra, the characteristic emission peaks of Pr^{3+} ions at 608 nm and 638 nm are observed, and therefore white light-emitting diodes (WLEDs) with improved color-rendering properties obtained by using modified Ce:Pr:YAG phosphors. The composite phase structure of ceramic phosphor is designed for improving the extraction efficacy and increasing the luminous efficacy by breaking the total internal reflection (TIR) at the interface between air and ceramic.

1. Introduction

YAG has been widely investigated for its applications in different fields, such as lasers, scintillators, and optical windows, because of its attractive optical properties, outstanding chemical stability, and high thermal resistance [1–3]. The application of Ce:YAG transparent ceramics to white light-emitting diodes (WLEDs) is also an important research interest.

Currently, commercial WLEDs combine a blue chip and yellow phosphor. However, the deterioration of polymers (epoxy or silicone) that encapsulate chips and phosphors raises several issues for practical applications of WLEDs, such as the degradation of luminous efficacy and alteration of color coordinates [4]. Inorganic block phosphor materials such as the Ce:YAG transparent phosphor ceramic are a promising candidate for realizing high-performance WLEDs [5,6]. However, WLEDs with the Ce:YAG transparent phosphor ceramic show a low color-rendering index (CRI) because of the lack of the red spectral component. In order to obtain the ideal white light, red-emitting ions such as Cr^{3+} and Pr^{3+} have been directly introduced to enhance the red emission of Ce:YAG phosphors [7–9]. In the YAG matrix, the characteristic emission peaks of Pr^{3+} ions at 608 and 638 nm can effectively supply the red emission, and furthermore Pr^{3+} also affects the emission peak of Ce^{3+} red-shift.

In this study, Ce:Pr:YAG transparent phosphor ceramics were fabricated by a solid-state reaction in a vacuum, and the influence of the Pr^{3+} ion on the crystal structure and luminescence properties was investigated. The energy transfer between Ce^{3+} and Pr^{3+} was also examined.

2. Experiment details

2.1. Fabrication of Ce:YAG and Ce: Pr:YAG

Ceramic samples with the chemical formula $(Ce_xPr_yY_{1-x-y})_3Al_5O_{12}$ were prepared by solid-state reaction at high temperature. High-purity powders of Y_2O_3 (99.999%), Al_2O_3 (99.999%), CeO_2 (99.99%), and Pr_6O_{11} (99.99%) were used as the raw materials; 0.1 wt% MgO and 0.4 wt% TEOS were used as the additives and the additives could promote the reaction densification [10]. A homogeneous slurry of the mixed raw materials was obtained by wet ball milling with ethanol for 12 h and then dried in an

* Corresponding author.
E-mail address: zhousm@siom.ac.cn (S. Zhou).

https://doi.org/10.1016/j.jallcom.2018.02.129
0925-8388/

oven at 70 °C. The obtained powders were uniaxially pressed into disks at 10 MPa and then isostatically cold-pressed at 210 MPa. The compacted disks were sintered at 700 °C for 4 h in air to remove organic materials and then sintered at 1700 °C for 10 h under a vacuum of 10^{-3} Pa. Transparent ceramics were obtained; these were then cut and polished to the appropriate thickness for producing white light on a blue LED chip. To avoid concentration self-quenching of Pr^{3+} ions [11], the doping concentration of Pr^{3+} was controlled within 0.5 at%. Table 1 presents the sample compositions.

2.2. Crystalline structure and optical characterization

The particle sizes of the raw materials were detected with a scanning electron microscope (SEM) (JSM-6510, JEOL, Japan) and Bettersize 2000 laser particle size distribution analyzer. The structure of the transparent ceramic was characterized by X-ray diffraction (XRD) with a Cu Kα radiation source (Ultima IV Diffractometer, Rigaku, Japan) in the angle range of $2\theta = 10°–90°$ at a scan step width of 0.02°. The fracture surface microstructure was also observed with the SEM (FESEM, HitachiS-4800, Japan), and grain sizes of the sintered samples were calculated by the linear intercept method from the SEM images of the fracture surfaces. The absorption spectrum was measured with UV/VIS/NIR spectrometry (Lambda 750, PerkinElmer, Inc., U.S.A.), and the scanning wavelength was measured from 200 nm to 600 nm. Emission spectra of samples with an excitation wavelength at 446 nm were obtained by using an integrating sphere (Everfine PMS-50 system) at the Shanghai Semiconductor Lighting Engineering Research Center, which was also used to evaluate the CRI and luminous efficacy. The fluorescence lifetime of Ce^{3+} at the fluorescence peak of 530 nm were measured under excitation of 460 nm by Edinburgh Instruments FLSP920 time resolved spectrometer.

Table 1
Compositions of the $(Ce_xPr_yY_{1-x-y})_3Al_5O_{12}$ transparent ceramics.

Sample number	P0	P1	P2	P3	P4
$x/(Ce_xPr_yY_{1-x-y})_3Al_5O_{12}$	0.1%	0.1%	0.1%	0.1%	0.2%
$y/(Ce_xPr_yY_{1-x-y})_3Al_5O_{12}$	0%	0.1%	0.3%	0.5%	0.2%

3. Results and discussion

3.1. Transparent ceramics and structural characterization

Fig. 1 shows the SEM micrographs and particle-size distributions of the starting powders as well as an SEM image of the ball-milled raw materials. The average particle sizes of the Y_2O_3 and Al_2O_3 powders were about 5.844 and 19.30 μm, respectively. The particle size distribution of Y_2O_3 was more concentrated, while that of Al_2O_3 was relatively dispersed, as shown in Fig. 1(d) and (e). The SEM image of the Y_2O_3 microstructure shows irregular particles and even edges and corners. However, the Al_2O_3 microstructure exhibits rounded corners. The different microstructures should be attributed to the different crystal structures of α-Al_2O_3 and cubic-Y_2O_3 crystallites and the different preparation methods. Al_2O_3 and Y_2O_3 were weighted in accordance with the stoichiometric ratio of YAG and mixed by wet ball milling. Then, the mixed powder was sintered at 700 °C in air to remove organic additives. The size of the mixed powder particles was 1–4 μm, as shown in Fig. 1(c). The sintering took place at 700 °C to avoid a reaction between Y_2O_3 and Al_2O_3 [12].

Fig. 2 shows the characteristic XRD patterns of the samples prepared by vacuum sintering. All peaks corresponded to the YAG phase, and no other phases were detected. This indicates that the samples were completely formed of a CeO_2–Pr_2O_3–YAG solid (see Fig. 3).

SEM micrographs of the Ce:Pr:YAG transparent ceramics with different Pr^{3+} concentrations indicated transgranular and intergranular fracture modes. A few pores at the grain boundaries and even in the grain were observed. During the solid-state reaction process, the radius of Al^{3+} (0.054 nm) was smaller than that of Y^{3+},

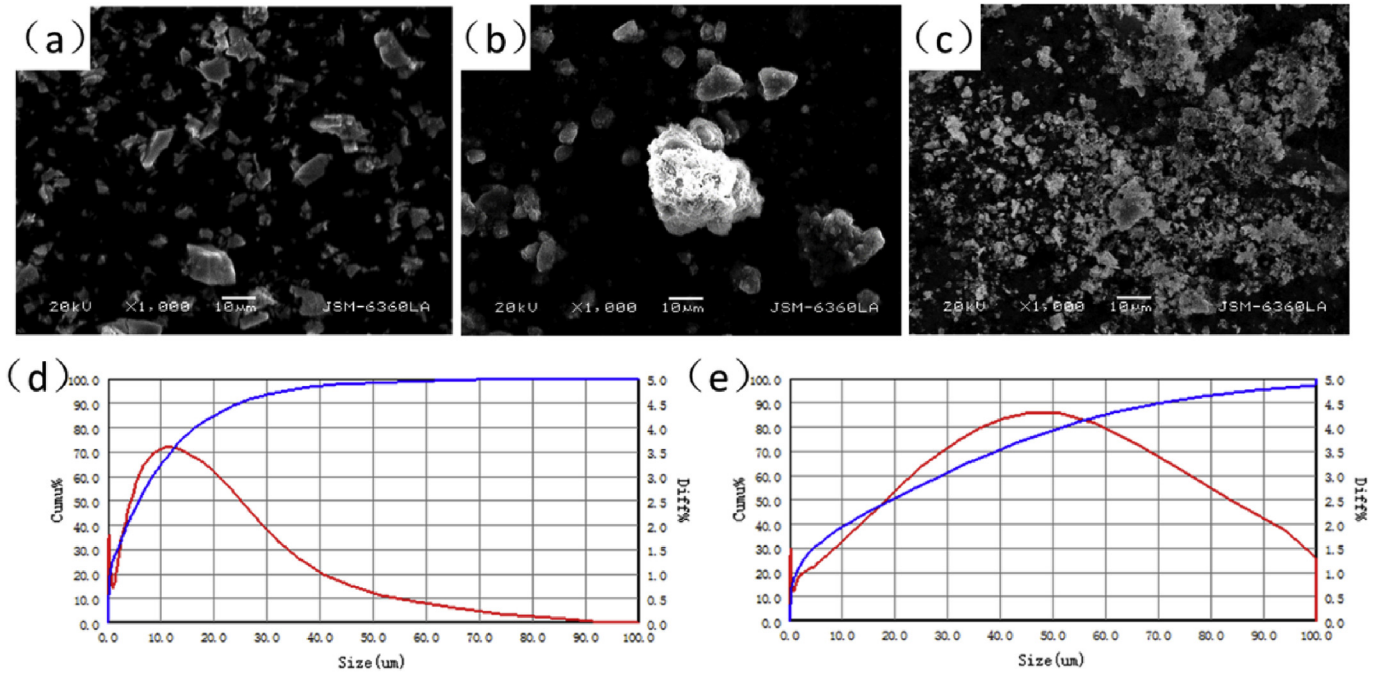

Fig. 1. SEM images of (a) Y_2O_3 powder, (b) Al_2O_3 powder, and (c) Y_2O_3 and Al_2O_3 mixed powder with YAG stoichiometric composition. Size distribution curves of (d) Y_2O_3 and (e) Al_2O_3.